Macromolecular Research

Article

DOI 10.1007/s13233-020-8107-z

www.springer.com/13233 pISSN 1598-5032 eISSN 2092-7673

Effects of Bulk Heterojunction Morphology Control *via* Thermal Annealing on the Fill Factor of Anthracene-based Polymer Solar Cells

Hyojung Cha[1]
Jiaqiang Li[2]
Yifan Li[2]
Seul-Ong Kim[2]
Yun-Hi Kim*[,3]
Soon-Ki Kwon*[,2]

[1] Department of Chemical Engineering, Pohang University of Science and Technology (POSTECH), Pohang 37673, Korea
[2] Department of Materials Engineering and Convergence Technology and ERI, Gyeongsang National University, Jinju 52828, Korea
[3] Department of Chemistry and ERI, Gyeongsang National University, Jinju 52828, Korea

Received October 29, 2019 / Revised December 17, 2019 / Accepted December 24, 2019

Abstract: Here we report a polymeric semiconductor (ODATT) comprising alkoxy anthracene (ODA) and thienothiophene (TT) polymerized by stille coupling reaction with the Pd catalyst. The optical properties of the polymer:$PC_{71}BM$ blend films are used by the UV-Visible absorption spectroscopy. The ODATT blends with $PC_{71}BM$ exhibit a maximal power conversion efficiency of 2.2% *via* thermal annealing treatment. Morphological analysis of the polymer:$PC_{71}BM$ blend films demonstrate the influence of ODATT polymer segregation on device performance by atomic force microscopy and transmission electron microscopy. We confirmed that ODATT has enhanced fill factor after thermal annealing treatment from the reduced series and shunt resistance from morphological enhancement.

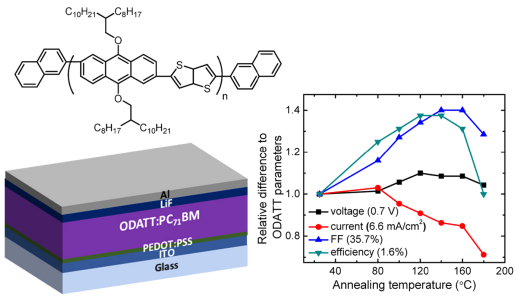

Keywords: organic solar cell, morphology, thermal treatment, anthracene, fill factor.

1. Introduction

Organic photovoltaic (OPV) devices have attracted significant attention due to their potential advantages over traditional silicon-based solar cells for solution-processed roll-to-roll device applications.[1-3] Moreover, large area, light, semi-transparent, and flexible OPV devices could be used in portable and wearable electronic devices.[4-6] All of the exceptional features of OPVs result from the materials used in their fabrication.[7-10] Currently, high-performance OPV devices are composed of a blend of conjugated small molecules or polymers as electron donors, and a fullerene derivative or nonfullerene small molecules as electron acceptors.[4,7,11-14] Despite significant progress in the material design of these photoactive layers, OPV performance is still not adequate for commercialization.

For improved photovoltaic performance, the OPV device operating mechanism must be better understood. Regarding the parameters used for determining photovoltaic performance, the fill factor (FF) is less understood and more complex than other key parameters, such as current density (JSC) and open-circuit voltage (V_{OC}).[15,16] The FF depends on charge carrier losses during charge generation, which occur due to exciton generation and diffusion, charge transfer, dissociation, transport, and collection by the electrodes.[10,17,18] To obtain a high FF in a photovoltaic device, photogenerated charge carriers must flow smoothly to the electrodes *via* a built-in potential generated by an applied bias.[18-20] However, for both OPV devices and other types of photovoltaic technology, the FF cannot reach 100% due to charge carrier losses occurring during device operation.

In most photovoltaic devices, photocurrent leakage results from electrical defects, such as pinholes and traps in the bulk, or occurs at the interfaces of layers, especially the interface between the photoactive layer and the electrodes. Additionally, due to a bulk heterojunction (BHJ) layer consisting of both donor and acceptor materials, OPV devices have complex donor-acceptor interfaces in the active layer, and between the active layer and electrodes. Therefore, most charge carrier losses are from the bulk of the active layer or occur due to contact between the active layer and electrode.[15,16] In practical photovoltaic devices, fine-tuning the domain size to suppress recombination can provide a high FF. Defects in the active layer, such as pinholes and traps, can act as recombination sites and also lead to current leakage. In optimized blends with minimal defects (achieved by fine-tuning the morphology), the excitons from the donor domain can readily diffuse toward the domain interface and separate into free charge carriers *via* a strong local field.[21-23] To enhance exciton separation yield and suppress donor/acceptor interfacial recombination in the bulk, the domain size should be within the exciton diffusion length, *i.e.*, up to 10-20 nm, for effective exciton separation at the donor/acceptor interface without exciton decay to the ground state. The domain size can be changed by varying the processing conditions, such as by thermal annealing,[24] solvent vapor annealing,[24] use of processing additives,[25] and alteration of the blend composition.[26] Conjugated polymers based on anthra-

Acknowledgment: This research was supported by the Technology Development Program to Solve Climate Changes of the National Research Foundation (NRF) funded by the Ministry of Science, ICT & Future Planning (No. 20161A2A2940911).

***Corresponding Authors:** Soon-Ki Kwon (skwon@gnu.ac.kr), Yun-Hi Kim (ykim@gnu.ac.kr)

cene have many advantages as electron-donating materials.[27,28] The anthracene structures are fused aromatic compounds that induce intermolecular interactions, leading to high charge-carrier mobility in organic field-effect transistors (OFETs). We previously reported naphthalene-based electron-donating polymers.[29] The series of polymers achieved a power conversion efficiency (PCE) of 4.15% with high V_{OC}. In this study, we used an anthracene-based conjugated polymer (ODATT) for an OPV application. We investigated the influence of blend morphology on device performance, and the impact of blend composition ratio and thermal treatment on FF. Although the anthracene structure showed lower solubility in organic solvents, the branched alkoxy side chain offset this. The anthracene-based molecule can be readily synthesized *via* simple purification for low-cost commercialization.

2. Experimental

2.1. Synthesis

All reactions were carried out under a nitrogen (N_2) atmosphere using standard Schlenk techniques. All chemical reagents were purchased from Aldrich and used as received.

2.1.1. Synthesis of 2,6-dibromo-9,10-bis(2-octyldodecyloxy) anthracene

The reaction followed the literature method.[28] The product was purified on a silica column using hexane as the eluent (yield: 75%). Proton nuclear magnetic resonance (^{1}H NMR) [300 MHz, $CDCl_3$, δ: 8.40 (d, 2H), 8.14 (d, 2H), 7.55 (d, 2H), 4.00 (d, 4H), 2.46 (m, 2H), 1.77 (m, 4H), 1.28 (m, 54H), 0.90 (m, 12H)]. Fast atom bombardment-mass spectrometry (FAB-MS): m/z: 929 (M^+).

2.1.2. Synthesis of 2,5-bis(trimethylstannyl)thieno[3,2-b] thiophene

An anhydrous tetrahydrofuran (THF) solution (2.00 g in 100 mL; 14 mmol) of thieno[3,2-b]thiophene was cooled to -78 °C under an N_2 atmosphere as reported previously.[30] A solution of 2.5 M n-butyl lithium in hexane (12 mL, 30 mmol) was added dropwise over 5 min, and the resulting solution was allowed to warm to room temperature with continuous stirring for 2 h. The resulting suspension was cooled to -78 °C and a solution of 1 M trimethyltin chloride in THF (5.9 g, 30 mmol) was added dropwise. The reaction mixture was allowed to warm to room temperature and stirred overnight. Water was added and the organic phase was twice extracted with ethyl acetate (50 mL). The organic layer was washed with brine (80 mL), dried over anhydrous sodium sulfate, filtered, and concentrated under reduced pressure. The resulting crude product was recrystallized from acetonitrile to obtain the product (yield: 90%). ^{1}H NMR [300 MHz, $CDC1_3$, δ=7.26 (s, 2H), 0.39 (s, 18H)].

2.1.3. Polymerization of ODATT

2,5-Bis(trimethylstannyl)thieno[3,2-b] thiophene (300 mg, 0.64 mmol) and benzo[1,2-b:4,5-b′]dithiophene (BDT) (590 mg, 0.64 mmol) were dissolved in 10 mL of toluene; the solution was flushed with argon (Ar) for 5 min, followed by the addition of 50 mg of $Pd(PPh_3)_4$. The mixture was again flushed with Ar for 20 min. The reaction solution was heated to reflux for 6 h. The reaction mixture was cooled to room temperature and added dropwise to 100 mL of methanol (MeOH). The precipitate was collected and further purified by Soxhlet extraction with MeOH, hexane, and chloroform ($CHCl_3$) in sequence. The $CHCl_3$ fraction was concentrated and added dropwise to MeOH. Subsequently, the precipitates were collected and dried under vacuum overnight to obtain the solid polymer (450 mg, 65% yield). The weight-average molecular weight (M_w) and polydispersity index (PDI) estimated by gel permeation chromatography (GPC) were 10.0 kDa and 1.18, respectively. ^{1}H NMR [500 MHz, $CDC1_3$, δ = 8.3-7.5 (br, 8H), 4.07-3.55 (br, 4H), 2.46 (m, 2H), 2.0-1.0 (br, 64H), 0.90 (m, 12H)].

3. Results and discussion

The synthesis of the anthracene-based conjugated polymer (ODATT) is illustrated in Scheme 1. The monomer was prepared by various reactions, such as bromination, nucleophilic substitution, and stannylation. The ODATT was polymerized by Stille coupling using Pd(0) catalyst under an N_2 atmosphere. After ODATT polymerization, end-capping was carried out with 2-bromonaphthalene and 2-stannyl-naphthalene. Oligomeric materials were removed from the crude polymer by Soxhlet extraction with acetone, hexane, MeOH, toluene, and $CHCl_3$ to provide dark red-colored polymers. The molecular structure was determined by ^{1}H NMR and infrared (IR) spectroscopic studies. The polymer ODATT with branched alkoxy side chain was highly soluble in most organic solvents, including $CHCl_3$ and o-dichlorobenzene. Gel permeation chromatography revealed that the polymer ODATT had a number-average molecular weight (Mn) of 8.5 kDa with a PDI of 1.18 with respect to polystyrene standard. Thermogravimetric analysis (TGA) was used to show that ODATT under N_2 atmosphere was thermally stable to 266°C. However, no transitions were observed by differential scanning calorimetry (DSC)

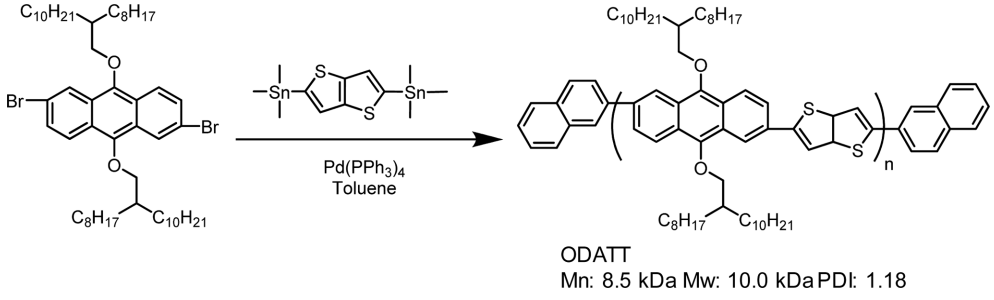

Scheme 1. Synthetic and polymeric route of ODATT.

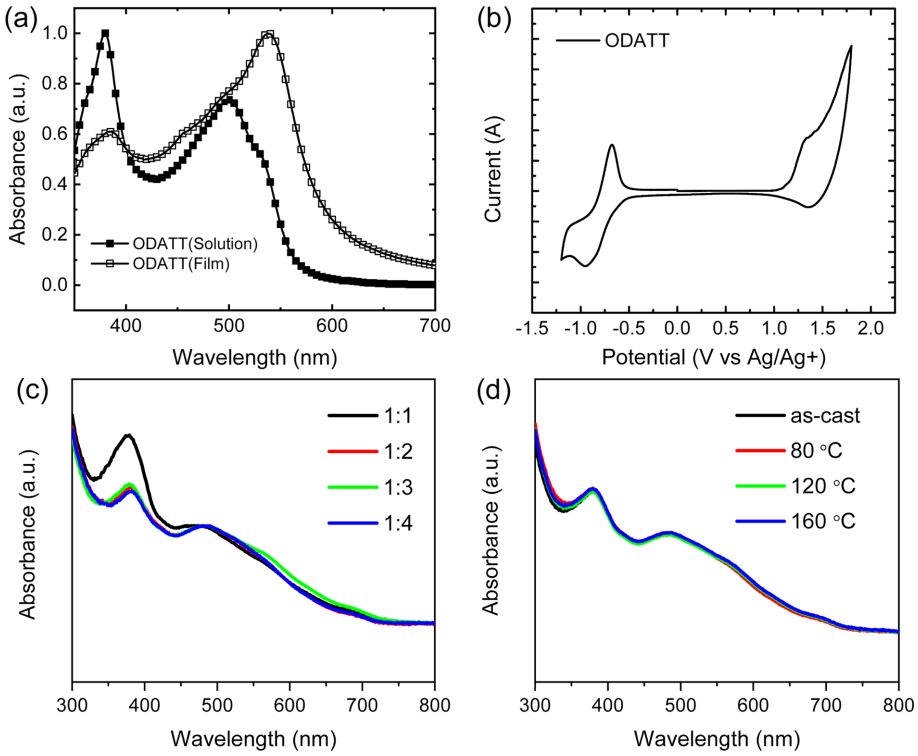

Figure 1. (a) UV-Vis absorption spectra of ODATT in solution ($CHCl_3$) and film. (b) Cyclic voltammetry of ODATT (c) UV-Vis absorption spectra of ODATT:$PC_{71}BM$ blend films with various composition ratios and (d) ODATT:$PC_{71}BM$ (1:3) blend films with various thermal annealing temperatures.

Table 1. Summary of optical and electrochemical properties of ODATT

	UV-S (max) (nm)	UV-F (max) (nm)	UV-edge (nm)	Band gap (optical) (eV)	LUMO (optical) (eV)	Oxidation onset (eV)	Reduction onset (eV)	LUMO (Electro-chemical) (eV)	HOMO (Electro-chemical) (eV)	Band gap (Electro-chemical) (eV)
ODATT	380, 499	384, 538	616	2.01	-3.54	1.13	-0.56	-3.86	-5.55	1.69

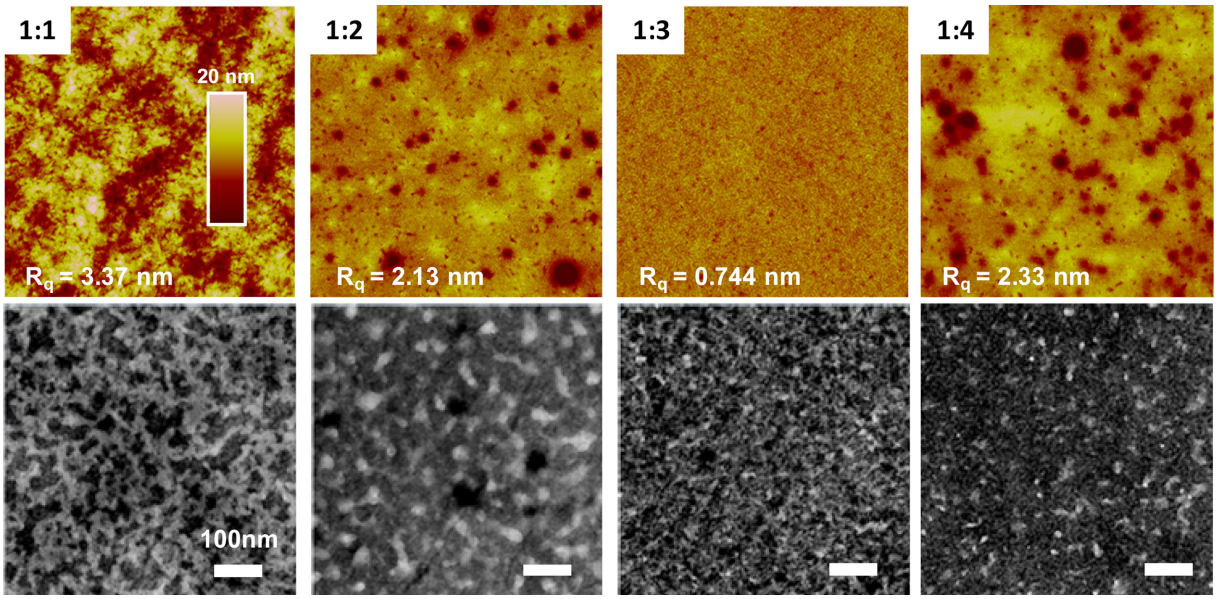

Figure 2. AFM (up) and TEM (down) images of ODATT blend films with $PC_{71}BM$.

(Figure S1).

The ultraviolet-visible absorption spectrum of a dilute solution of ODATT in $CHCl_3$ (Figure 1 and Table 1) exhibited broad absorption, with λ_{max} at 499 nm. The ODATT film showed maximum absorption at 538 nm, red-shifted by 61 nm compared with that of a dilute solution. Cyclic voltammetry (CV) was used to investigate the energy levels of the ODATT polymer. The highest-occupied molecular orbital (HOMO) and lowest-unoccupied molecular orbital (LUMO) levels of ODATT were estimated using a previously reported empirical equation[31] and are sum-

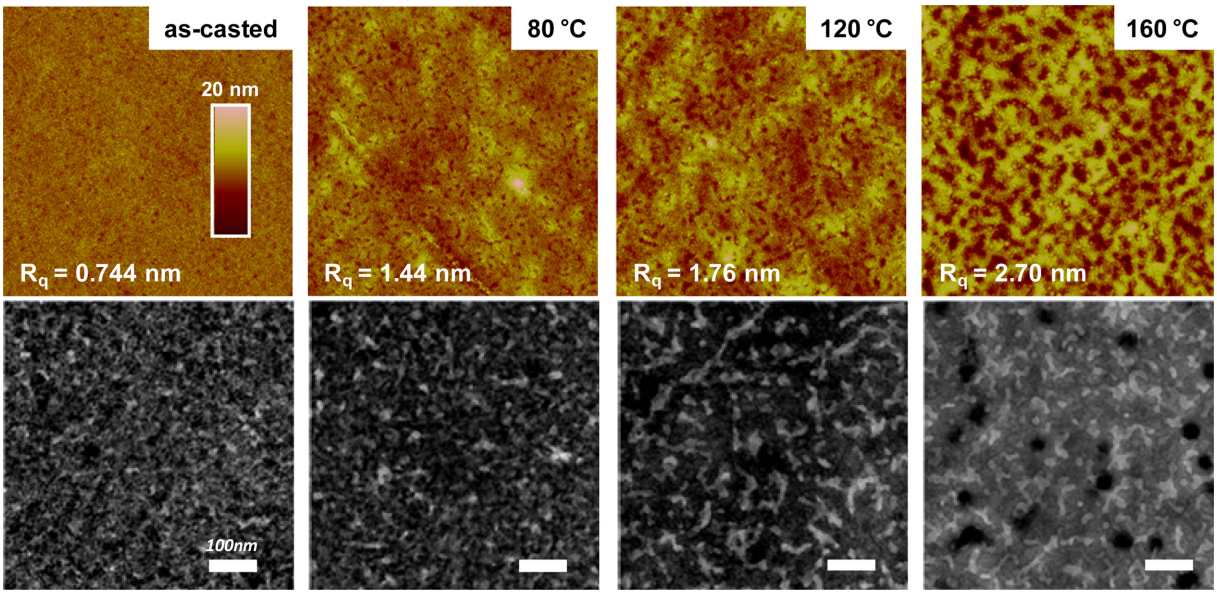

Figure 3. AFM and TEM images of ODATT blend films with $PC_{71}BM$ with/without thermal treatment up to 160 °C.

marized in Figure 1 and Table 1. The calculated HOMO level of ODATT was -5.5 eV, which is much lower than that of poly(3-hexylthiophene) (P3HT) (-4.9 eV) and led to higher oxidation stability and V_{OC}.[32] The polymer structure was also investigated by density functional theory (DFT) (Figure S2). The structure derived from the DFT calculations showed weak intermolecular interactions in ODATT due to branched alkoxy chains preventing interdigitation.[29] At the HOMO and LUMO energy levels, electrons were almost delocalized in the anthracene and thiophene units.

To investigate the morphology of the photoactive layer, all of the films were prepared by dissolving a blend of ODATT with [6,6]-phenyl C_{71}-butyric acid methyl ester ($PC_{71}BM$) at four weight ratios (1:1 to 1:4) in dichlorobenzene, followed by spin-coating on the top surface of a poly(3, 4-ethylenedioxythiophene): poly(styrene sulfonate) (PEDOT:PSS) film on indium-tin oxide (ITO)-patterned glass substrate. The prepared films were annealed at different temperatures up to 180 °C on a hot plate under an N_2 atmosphere. We observed the top surface of the ODATT:$PC_{71}BM$ blend films using atomic force microscopy (AFM) in tapping mode (Figure 2). The ODATT:$PC_{71}BM$ film prepared at the 1:3 weight ratio exhibited a relatively smooth and homogeneous surface, with a low roughness of 0.744 nm. The other blend film samples prepared at the 1:1, 1:2, and 1:4 ratios showed micron-sized grains with significant phase separation. The AFM images (tapping mode) of the ODATT:$PC_{71}BM$ blend films prepared at the various donor:acceptor ratios were notably different in terms of morphology. After thermal annealing, well-segregated domains were observed in the ODATT (Figure 3). Unannealed ODATT had a smooth and well-mixed morphology. However, domains increased in size with increasing annealing temperature. Transmission electron microscopy (TEM) was used to analyze the bulk morphology of these films. Thermal annealing caused the polymer phase to increase (bright phase in the images). We investigated device performance according to blend morphology.

Figure 4 shows the performance of the OPV device fabricated with an active layer of ODATT:$PC_{71}BM$. Dichlorobenzene was used as the solvent to prepare high-quality films.

The current-voltage (*J-V*) curves of the optimized photovoltaic devices with various composition ratios are shown before and after annealing at 180 °C for 30 min. The device parame-

Table 2. Photovoltaic performances of organic photovoltaic cells based on blends of ODATT with $PC_{71}BM$ under the illumination of AM1.5G, 100 $mWcm^{-2}$

D:A Ratio	Annealing temperature (°C)	Solar cell performance			
		V_{OC} (V)	J_{SC} (mA/cm^2)	FF (%)	PCE (%)
1:1	As	0.65	3.2	29.3	0.6
1:2		0.70	4.3	24.8	0.73
1:3		0.70	6.6	35.7	1.6
1:4		0.79	3.7	33.2	0.96
1:3	As	0.70	6.6	35.7	1.6
	80	0.71	6.8	41.4	2.0
	100	0.74	6.3	45.4	2.1
	120	0.77	6.0	47.9	2.2
	140	0.76	5.7	50.0	2.2
	160	0.76	5.6	50.0	2.1
	180	0.73	4.7	45.9	1.6

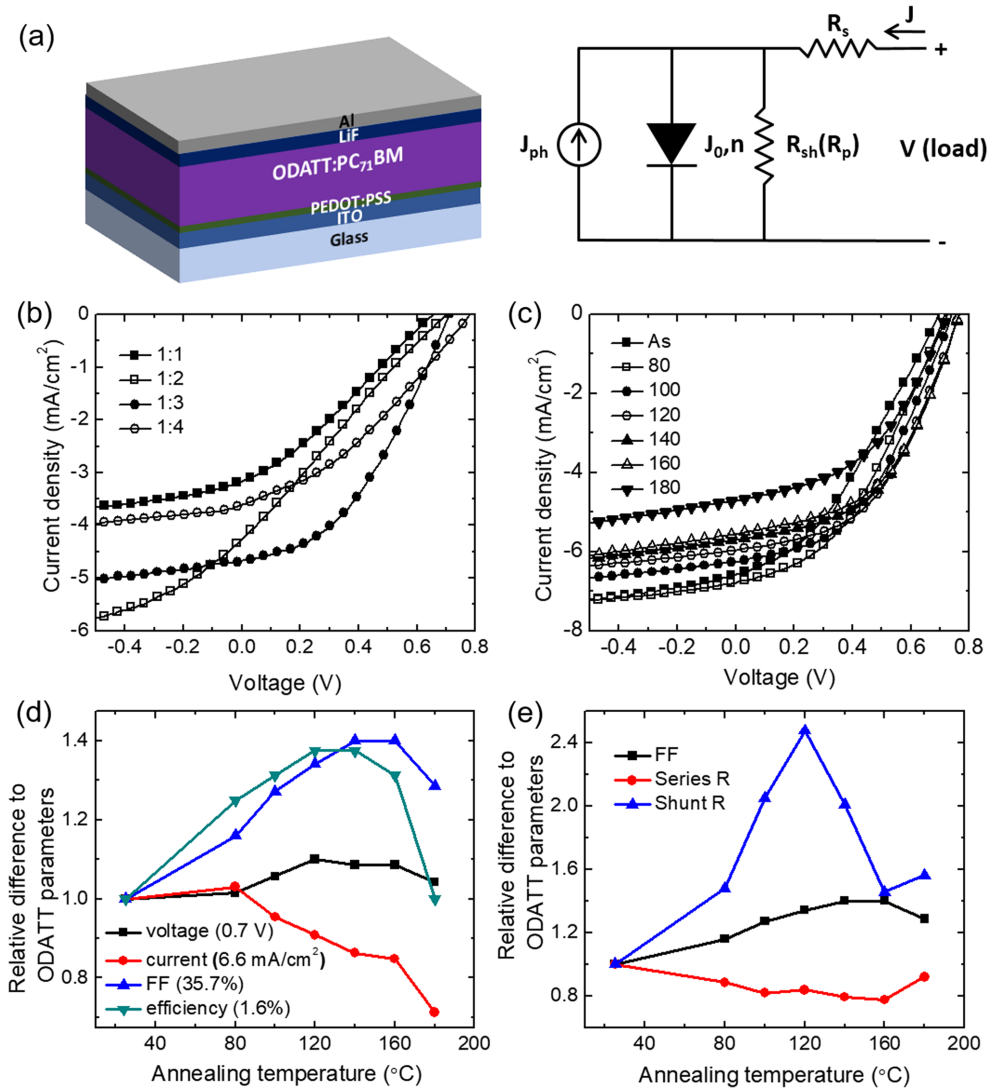

Figure 4. (a) Device structure used in this study and equivalent circuit of photovoltaic cell, *J-V* curves of organic photovoltaic cells based on the ODATT (donor) and $PC_{71}BM$ (acceptor) blends under the illumination of AM1.5G, 100 $mWcm^{-2}$ (b) with various donor:acceptor weight ratios and (c) with increasing annealing temperature at 1:3 ratio. (d) Relative device performance parameters and (e) relative resistance parameters as a function of annealing temperatures.

ters are summarized in Table 2. The as-cast ODATT-based OPV device exhibited a JSC of 6.6 mA cm^{-2}, V_{OC} of 0.70 V, FF of 35%, and PCE of 1.6% at the 1:3 ratio. After annealing, OPV device performance improved to a JSC of 6.8 mA cm^{-2}, V_{OC} of 0.76 V, FF of 50%, and PCE of 2.2%. Thermal annealing enhanced mainly V_{OC} and FF through reduced series and shunt resistance due to ODATT polymer segregation (Figure 4).

The increased PCE resulted from improved morphology. This new semiconducting polymer with alternating alkyloxyanthracene and thienothiophene units was thus synthesized and characterized. Due to the superior miscibility of ODATT and $PC_{71}BM$, a homogeneous morphology was achieved at the 1:3 blend ratio, and the resulting blend yielded a PCE of 1.6% and V_{OC} of 0.7 V.

Moreover, the OPV device was optimally annealed at 120-160 °C to provide a PCE of 2.2%. This device showed better nanoscale segregation of the ODATT polymer, which led to enhanced FF due to reduced series and shunt resistance.

4. Conclusions

New semiconducting polymer with alternating alkyloxyanthracene and thienothiophene units was synthesized and characterized. The ODATT:$PC_{71}BM$ film prepared at the 1:3 weight ratio exhibited a relatively smooth and homogeneous surface, with a low roughness of 0.744 nm., and the resulting blend yielded a PCE of 1.6% and a VOC of 0.7 V. Moreover, the OPV device was optimally annealed at 120-160 °C to provide a PCE of 2.2%. This device showed better nanoscale segregation of the ODATT polymer, which led to enhanced FF due to reduced series and shunt resistance.

Supporting information: Information is available regarding the thermogravimetric analysis (TGA), differential scanning calorimetry (DSC) and DFT calculation of ODATT. The materials are available *via* the Internet at http://www.springer.com/13233.

References

(1) W. Xu and F. Gao, *Mater. Horizons,* **5**, 206 (2018).
(2) L. Meng, Y. Zhang, X. Wan, C. Li, X. Zhang, Y. Wang, X. Ke, Z. Xiao, L. Ding, R. Xia, H.-L. Yip, Y. Cao, and Y. Chen, *Science,* **361**, 1094 (2018).
(3) J. Liu, S. Chen, D. Qian, B. Gautam, G. Yang, J. Zhao, J. Bergqvist, F. Zhang, W. Ma, H. Ade, O. Inganäs, K. Gundogdu, F. Gao, and H. Yan, *Nat. Energy*, **1**, 16089 (2016).
(4) S. Dai and X. Zhan, *Adv. Energy Mater.,* **8**, 1 (2018).
(5) H. Hu, P. C. Y. Chow, G. Zhang, T. Ma, J. Liu, G. Yang, and H. Yan, *Acc. Chem. Res,.* **50**, 2519 (2017).
(6) F. Laquai, D. Andrienko, C. Deibel, and D. Neher, in *Elementary Processes in Organic Photovoltaics,* Advances in Polymer Science Series, Springer, 2017, Vol. 272, pp 267-291.
(7) Q. Wang, Y. Li, P. Song, R. Su, F. Ma, and Y. Yang, *Polymers (Basel),* **9**, 692 (2017).
(8) G. J. Hedley, A. Ruseckas, and I. D. W. Samuel, *Chem. Rev.,* **117**, 796 (2017).
(9) V. V. Brus, J. Lee, B. R. Luginbuhl, S.-J. Ko, G. C. Bazan, and T.-Q. Nguyen, *Adv. Mater.,* **31**, 1900904 (2019).
(10) C. Poelking and D. Andrienko, *J. Am. Chem. Soc.,* **137**, 6320 (2015).
(11) Y. Lin, F. Zhao, Y. Wu, K. Chen, Y. Xia, G. Li, S. K. K. Prasad, J. Zhu, L. Huo, H. Bin, Z.-G. Zhang, X. Guo, M. Zhang, Y. Sun, F. Gao, Z. Wei, W. Ma, C. Wang, J. Hodgkiss, Z. Bo, O. Inganäs, Y. Li, and X. Zhan, *Adv. Mater.,* **29**, 1604155 (2017).
(12) J. Zhang, L. Zhu, and Z. Wei, *Small Methods,* **1**, 1700258 (2017).
(13) D. Qian, Z. Zheng, H. Yao, W. Tress, T. R. Hopper, S. Chen, S. Li, J. Liu, S. Chen, J. Zhang, X.-K. Liu, B. Gao, L. Ouyang, Y. Jin, G. Pozina, I. A. Buyanova, W. M. Chen, O. Inganäs, V. Coropceanu, J.-L. Bredas, H. Yan, J. Hou, F. Zhang, A. A. Bakulin, and F. Gao, *Nat. Mater.,* **17**, 703 (2018).
(14) Q. Fan, Y. Wang, M. Zhang, B. Wu, X. Guo, Y. Jiang, W. Li, B. Guo, C. Ye, W. Su, J. Fang, X. Ou, F. Liu, Z. Wei, T. C. Sum, T. P. Russell, and Y. Li, *Adv. Mater.,* **30**, 1704546 (2018).
(15) B. Qi and J. Wang, *Phys. Chem. Chem. Phys.,* **15**, 8972 (2013).
(16) M. H. Jao, H. C. Liao, and W. F. Su, *J. Mater. Chem. A,* **4**, 5784 (2016).
(17) J. Yu, Y. Zheng, and J. Huang, *Polymers (Basel),* **6**, 2473 (2014).
(18) I. Ramirez, M. Causa', Y. Zhong, N. Banerji, and M. Riede, *Adv. Energy Mater.,* **8**, 1703551 (2018).
(19) T. Kirchartz, P. Kaienburg, and D. Baran, *J. Phys. Chem. C,* **122**, 5829 (2018).
(20) P. Kaienburg, U. Rau, and T. Kirchartz, *Phys. Rev. Appl.,* **6**, 024001 (2016).
(21) C. Groves, *Energy Environ. Sci.,* **6**, 1546 (2013).
(22) F. C. Jamieson, E. B. Domingo, T. McCarthy-Ward, M. Heeney, N. Stingelin, and J. R. Durrant, *Chem. Sci.,* **3**, 485 (2012).
(23) S. Shoaee, S. Subramaniyan, H. Xin, C. Keiderling, P. S. Tuladhar, F. Jamieson, S. A. Jenekhe, and J. R. Durrant, *Adv. Funct. Mater.,* **23**, 3286 (2013).
(24) S. D. Collins, N. A. Ran, M. C. Heiber, and T. Q. Nguyen, *Adv. Energy Mater.,* **7**, 1602242 (2017).
(25) L. Ye, W. Zhao, S. Li, S. Mukherjee, J. H. Carpenter, O. Awartani, X. Jiao, J. Hou, and H. Ade, *Adv. Energy Mater.,* **7**, 1602000 (2017).
(26) H. B. Naveed and W. Ma, *Joule,* **2**, 621 (2018).
(27) D. S. Chung, J. W. Park, S.-O. Kim, K. Heo, C. E. Park, M. Ree, Y.-H. Kim, and S.-K. Kwon, *Chem. Mater.,* **21**, 5499 (2009).
(28) J. Y. Ma, H.-J. Yun, S.-O. Kim, G. B. Lee, H. Cha, C. E. Park, S.-K. Kwon, and Y.-H. Kim, *J. Polym. Sci. Part A Polym. Chem.,* **52**, 1306 (2014).
(29) S.-O. Kim, D. S. Chung, H. Cha, M. C. Hwang, J.-W. Park, Y.-H. Kim, C. E. Park, and S.-K. Kwon, *Sol. Energy Mater. Sol. Cells,* **95**, 1678 (2011).
(30) C. W. Jeon, S.-H. Kang, H.-J. Yun, T. K. An, H. Cha, C.-E. Park, and Y.-H. Kim, *Synth. Met.,* **185-186**, 159 (2013).
(31) H. Cha, G. Fish, J. Luke, A. Alraddadi, H. H. Lee, W. Zhang, Y. Dong, S. Limbu, A. Wadsworth, I. P. Maria, L. Francàs, H. L. Sou, T. Du, J.-S. Kim, M. A. McLachlan, I. McCulloch, and J. R. Durrant *Adv. Energy Mater.,* **9**, 1901254 (2019).
(32) S. Holliday, R. S. Ashraf, A. Wadsworth, D. Baran, S. A. Yousaf, C. B. Nielsen, C.-H. Tan, S. D. Dimitrov, Z. Shang, N. Gasparini, M. Alamoudi, F. Laquai, C. J. Brabec, A. Salleo, J. R. Durrant, and I. McCulloch, *Nat. Commun.,* **7**, 11585 (2016).

